Perfect acoustic absorption in reciprocal ventilated problems

Vicente Romero-García[1,*], Noé Jiménez[2], Vincent Pagneux[1] and Jean-Philippe Groby[1]

[1]Laboratoire d'Acoustique de l'Université du Mans (LAUM), UMR 6613, Institut d'Acoustique - Graduate School (IA-GS), CNRS, Le Mans Université, Le Mans, France.
[2]Instituto de Instrumentación para Imagen Molecular (I3M), Universitat Politècnica de València - CSIC, València, Spain.

*{vicente.romero@univ-lemans.fr}

Abstract
This work presents the different possibilities to obtain perfect absorption in reciprocal ventilated problems, i.e., in the situation in which both reflection and transmission are considered. By using the scattering matrix formalism, the perfect absorption is obtained when the critical coupling conditions are fulfilled, i.e., when the two eigenvalues of the scattering matrix are zero at the same frequency and the system is excited with the corresponding eigenvector. These conditions impose that only two types of mechanisms can be used to obtain perfect absorption: (i) breaking the symmetry by using non-symmetric resonators or (ii) maintaining the symmetry, but using degenerate resonators. We show two systems made of Helmholtz resonators presenting perfect acoustic absorption, each based on each solution. The systems are analytically, numerically, and experimentally characterized with a very good agreement between them, thus opening new venues for the design of acoustic treatments at low frequencies.

Keywords: Acoustic absorption, Perfect absorption, Critical coupling, Impedance matching.

1 Introduction

The ability to perfectly absorb an incoming wave field by a sub-wavelength material is advantageous for several applications in wave physics. This challenge requires to solve a complex problem: reducing the geometric dimensions of the structure while increasing the density of states at low frequencies and finding the good conditions to match the impedance to the background medium. A successful approach for increasing the density of states at low frequencies with reduced dimensions is the use of metamaterials. Several possibilities based on these systems made of open lossy resonant building blocks have been proposed to design sound absorbing structures which can present simultaneously sub-wavelength dimensions and strong acoustic absorption [1, 2]. Among them, Helmholtz resonators (HRs) have been shown as potential candidates to solve the problem due to the tunable possibilities they offer [1, 2, 3, 4, 5, 6, 7, 8, 9, 10].

In this talk we want to pay attention to the possibilities provided by the acoustic metamaterials to *perfectly* absorb waves with deep sub-wavelength dimensions in the ventilated problem, i.e., in a transmission problem in which we consider both reflection and transmission. From a general point of view, the perfect absorption can be analyzed from the interaction of an incoming wave with an open, lossy and resonant structure. In particular the impedance matching with the background field, is one of the most studied process in the field of wave physics [11, 12, 13]. These open systems, at the resonant frequency, are characterized by both the leakage rate of energy (i.e., the coupling of the resonant elements with the propagating medium), and the intrinsic losses of the resonator. The balance between the leakage and the losses activates the condition of critical coupling (or impedance matching condition), trapping the energy around the resonant elements and generating a maximum of energy absorption [3, 14]. In the case of transmission systems, degenerate critically coupled resonators with symmetric and antisymmetric resonances or systems with broken symmetry can be used to perfectly absorb the incoming energy.

2 Theoretical framework

Let us consider a two-port, one-dimensional and reciprocal scattering process. The relation between the amplitudes of the incoming (a, d), and outcoming (b, c) waves, on both sides of an asymmetric (non-mirror symmetric) scatterer Σ, is given by

$$\begin{pmatrix} c \\ b \end{pmatrix} = \mathbf{S}(f)\begin{pmatrix} a \\ d \end{pmatrix} = \begin{pmatrix} T & R^+ \\ R^- & T \end{pmatrix}\begin{pmatrix} a \\ d \end{pmatrix}, \tag{1}$$

where $\mathbf{S}(f)$ is the scattering matrix (S-matrix), f is the incident wave frequency, T is the complex transmission coefficient, R^- and R^+ are the complex reflection coefficients for left ($-$) and right (+) incidence, respectively. In this work, the time dependence convention of the harmonic regime is $e^{-i\omega t}$, and it will be omitted in the following. The eigenvalues of the $\mathbf{S}$-matrix are expressed as $\lambda_{1,2} = T \pm [R^-R^+]^{1/2}$ and the eigenvectors of the system are $\mathbf{v_1} = (v_{11}, v_{12}) = \left(R^+, -\sqrt{R^+R^-}\right)$ and $\mathbf{v_2} = (v_{21}, v_{22}) = \left(\sqrt{R^+R^-}, R^+\right)$. Therefore, the ratio of the eigenvector components v_{1i} and v_{2i} is $v_{2i}/v_{1i} = (-1)^i(R^-/R^+)^{1/2}$. A zero eigenvalue of the $\mathbf{S}$-matrix corresponds to the case in which the incident waves can be completely absorbed ($b = c = 0$). This, called coherent perfect absorption (CPA) [15], happens when $T = \pm[R^-R^+]^{1/2}$ and the incident waves a, d correspond to the relevant eigenvector.

If the scatterer Σ is mirror symmetric, $R^+ = R^- \equiv R$ and the problem can be reduced to two uncoupled sub-problems by choosing incident waves that are symmetric or antisymmetric with the reflection coefficients $R_s = R + T$ and $R_a = R - T$. In particular, the reflection and transmission coefficients of the initial problem can be expressed as $R = (R_s + R_a)/2$, and $T = (R_s - R_a)/2$ while the eigenvalues of the $\mathbf{S}$-matrix can be written as $\lambda_1 = R_s$ and $\lambda_2 = -R_a$. For an one-sided incident wave, the absorption coefficient defined as $\alpha = 1 - |R|^2 - |T|^2$ becomes $\alpha = (\alpha_s + \alpha_a)/2$, where $\alpha_s \equiv 1 - |R_s|^2$ and $\alpha_a \equiv 1 - |R_a|^2$. Achieving $\alpha(f_{max}) = 1$ at a frequency f_{max}, is equivalent to getting simultaneously the minima of the reflection coefficients of the two sub-problems, i.e., $R_a(f_{max}) = R_s(f_{max}) = 0$ [$\alpha_s(f_{max}) = \alpha_a(f_{max}) = 1$]. This has been achieved in Ref. [16] for a mirror symmetric slab through intensive numerical calculations.

3 Perfect and broadband absorption in asymmetric resonators: Rainbow-trapping absorbers

In this section we analyze the scattering properties of a system made of N different HRs embedded in a waveguide. Due to the different HRs, the S-matrix is not symmetric and the scattering properties from both sides of the system must be analyzed. We start analyzing a system made of $N = 2$ HRs, considering the two directions of incidence, namely *forward* and *backward*, as depicted in Figs. 1 (a,b). The n-th resonator of the system presents a resonant frequency at f_n. Figures 1 (c-f) show the corresponding absorption, reflection and transmission coefficients for each case. [1]

First, in the forward configuration, shown in Fig. 1 (a), above f_1, a band gap is introduced and the transmission is strongly reduced, the HR acting effectively as a rigidly-backed wall for the right ingoing waves. Then, the resonator $n = 2$, with $f_2 > f_1$, is tuned to impedance match the system with the exterior medium at frequency f_{PA}, between f_1 and f_2. At this particular frequency, no reflected waves are produced and therefore, $\alpha = 1 - |R^-|^2 - |T|^2 = 1$ holds. As shown in Ref. [6] the optimization process looks for the geometry that introduce the good amount of viscothermal losses to minimize $\varepsilon(f_{PA}) = |R^-(f_{PA})|^2 + |T(f_{PA})|^2$ that maximizes the absorption at f_{PA}. In this situation, unidirectional perfect absorption is observed. The optimization of the geometry of the system, shows that a deep sub-wavelength panel with a thickness 40 times smaller that the wavelength can be designed [6]. It is worth noting here that the change of section in the main waveguide helps to achieve the impedance matching, specially for very thin systems as the one presented here.

[1] The results are calculated analytically using the transfer matrix method (TMM) in which the thermoviscous losses are accounted for, numerically using finite element method (FEM) and experimentally validated using stereo-lithographic 3D printed structures and impedance tube measurements. Details can be found in Ref. [6].

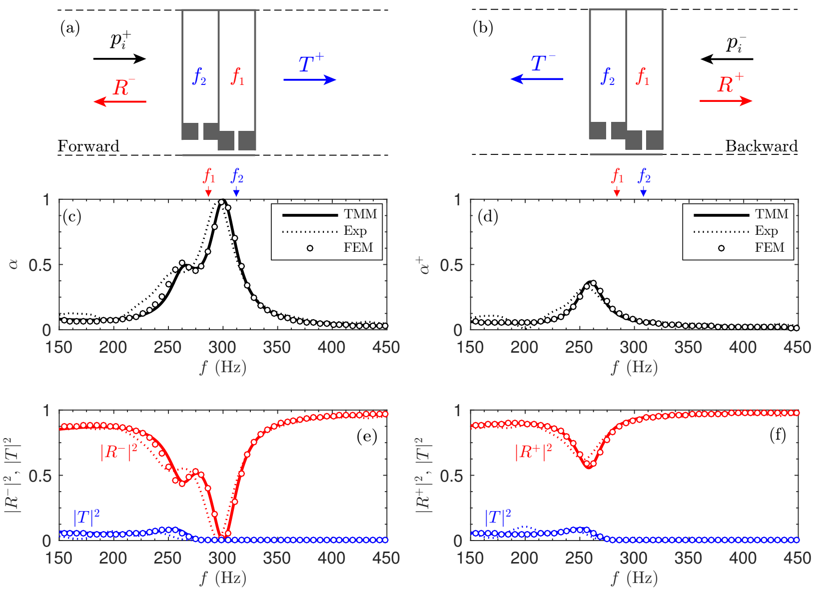

Figure 1: Scheme of the sub-wavelength non-mirror symmetric panel in (a) forward and (b) backward configuration. (c) Absorption for the forward configuration obtained using TMM (continuous line), FEM (circles), and experiment (dotted line). (e) Corresponding reflection and transmission coefficients. (d) Absorption for the backward configuration. (f) Corresponding reflection and transmission coefficients. The arrows mark the resonance frequencies of the HRs, f_1 and f_2. Figure adapted with permission from Ref. [6].

Second, in the backward propagation shown in Fig. 1 (b), the wave impinges first the lowest resonance frequency resonator from the right, f_1. Now at this frequency almost no transmission is allowed in the waveguide. As the waveguide is not impedance matched at f_1 in backward direction, reflection is high and absorption is poor ($\alpha^+ = 0.05$). For frequencies below f_2, propagation is allowed in the main waveguide and the effect of the second HR may be visible inducing a decrease of the reflection coefficient. However, the impedance matching in the backward direction is not fully achieved and only a small amount of absorption is observed near the resonance frequency of the first resonator.

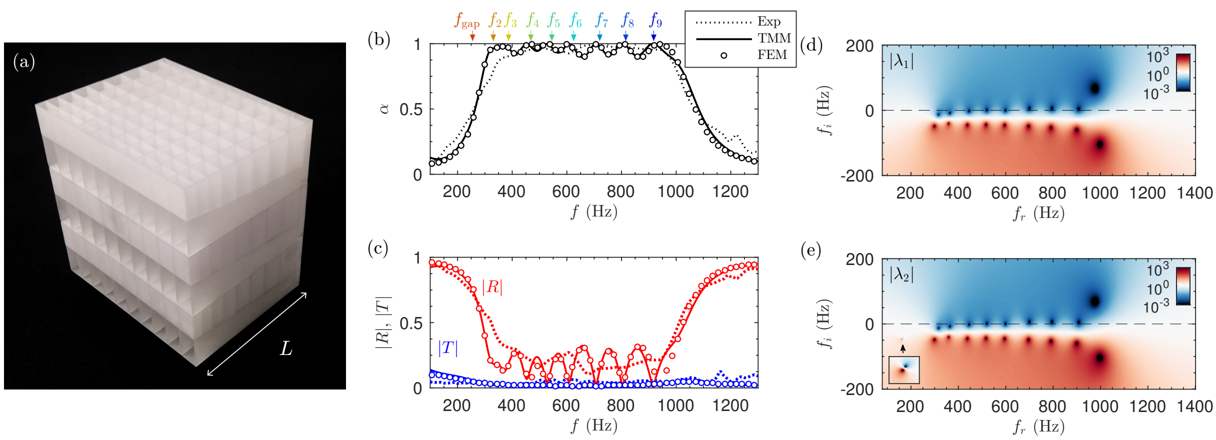

Figure 2: (a) Photograph of the sample containing 10×3 unit cells. (b) Absorption obtained by using the TMM (continuous line), FEM simulations (circles) and measured experimentally (dotted line). (b) Corresponding reflection (red curves) and transmission (blue curves) coefficients in amplitude. (d-e) Complex frequency representation of the eigenvalues of the scattering matrix, $\lambda_{1,2}$. Colormap in $10 \log_{10} |\lambda|^2$ scale. Figure adapted with permission from Ref. [6].

The concept previuosly described can be applied to design broadband perfect absorbers. The idea is to create a frequency-cascade of band-gaps and critically coupled resonators in order to generate a rainbow-trapping effect. We have designed a rainbow-trapping absorber (RTA) using $N = 9$ HRs and quantizing the dimensions of all the geometrical elements that compose the structure to the 3D machine precision. More details are given in Ref. [6]. The manufactured sample is shown in Fig. 2 (a). Figures 2 (b-c) show the absorption, reflection and transmission of the device.[2] The deepest resonator ($n = 1$) presents a resonance frequency of $f_1 = f_{\text{gap}} = 259$ Hz, causing the transmission to drop. A set of 8 resonators were tuned following the process previously described, with increasing resonance frequencies ranging from 330 to 917 Hz. As a result of the frequency-cascade process, the impedance of the structure in the working frequency range is matched with the exterior medium while the transmission vanishes. As a consequence, the RTA presents a flat and quasi-perfect absorption coefficient in this frequency range (see Fig. 2 (b)). It can be observed that at low frequencies there are small differences between the measurements and the models. These disagreements are mainly caused by imperfections in the sample manufacturing, by imperfect fitting of the structure to the impedance tube, by the possible evanescent coupling between adjacent waveguides and adjacent HRs, and/or by the limitations of the visco-thermal model used at the joints between waveguide sections.

The corresponding representation of the the two eigenvalues of the S-matrix in the complex frequency plane is shown in Figs. 2 (d-e). We can see that even under the constraints imposed by the metamaterial construction process, all the $N-1$ zeros of the eigenvalues that produce the critical coupling of the structure are located very close to the real frequency axis being the zeros of λ_1 at the same frequencies as those of λ_2. Note in the manufactured system, not all the zeros are located exactly on the real axis, but the quality factor of the resonances is very low, therefore they overlap producing quasi-perfect sound absorption in a frequency band from 300 to 1000 Hz for a panel 10 times thinner than the wavelength at 300 Hz in air.

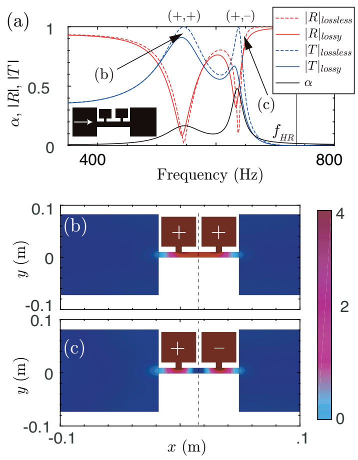

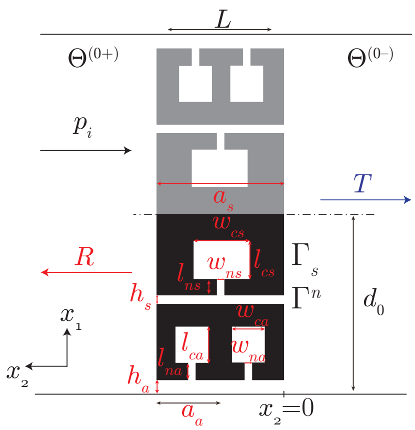

Figure 3: (a) shows the lossless (dashed lines) and lossy (continuous lines) scattering coefficients for the case of a slit loaded by two identical resonators (red lines correspond to the reflection coefficient while blue lines for the transmission one. Black lines represent the absorption coefficient for the lossy case). Inset shows the schema of the scattering problem, with the incident direction indicated with the withe arrow. Vertical black dashed line shows the symmetry plane of the resonator. (b) and (c) represent the absolute value of the total pressure field for the two first resonances of the slit loaded with two identical resonators. Vertical black dashed line shows the symmetry plane of the resonator. Figure adapted with permission from Ref. [17]. (d) Scheme of the mirror-symmetric building block used in this work with the definitions of the geometrical parameters. Figure adapted with permission from Ref. [17].

[2] Details of the modeling by the TMM, FEM and also of the experimental set-up are given in Ref. [6]

4 Perfect absorption with mirror symmetric resonators

Let us start the discussion by analyzing the scattering coefficients of a system made of a slit loaded with N resonators. This system presents N resonances. For simplicity but without loss of generality we analyze here the case with $N = 2$ in which the resonance frequency of the HRs is f_{HR}. we analyze the propagation through a slit loaded by two HRs as shown in the inset of the Fig. 3(a). In this case the scattering coefficients are plotted in Fig. 3(b), showing two transmission peaks corresponding to the first two Fabry-Perot resonances of the slit. The two first resonances of the slit are clearly visible on Figs. 3(b,c) that depict the absolute value of the total pressure field at these particular frequencies. The first mode is symmetric while the second mode is antisymmetric with respect to the symmetry plane of the system (shown by the dashed line in Figs. 3(b,c)).

Previous discussion allows us to conclude that resonators with symmetric and antisymmetric resonances can be designed with the combination of the discussed systems: a periodic arrangement of two slits loaded respectively with one and two HRs. As a consequence, the resonator design that we propose now, shown in Fig. 3(d), is a combination of slits loaded by one and two resonators. The slit loaded by a single resonator only supports symmetric modes, and will thus be named symmetric slit. The slit loaded by two resonators supports both symmetric and antisymmetric modes. It will be mainly used to tune the antisymmetric resonance and will thus be named antisymmetric slit. The geometric parameters of the degenerate resonator are defined in Fig. 3(d). The subindex s (a) represents the parameters for the symmetric (antisymmetric) slit.

In the previous section we have critically coupled the symmetric and the antisymmetric reflection subproblems. This means that the two eigenvalues of the scattering matrix vanish at the same frequency for the full transmission problem with the optimized geometry. Therefore, the full problem is critically coupled and perfect absorption is expected. Details of the geometry obtained from the optimization problem for the complete resonator can be found in Ref. [17].

Figure 4(a) shows the scattering coefficients of the full transmission problem. The agreement between the model, the numerical simulations and the experimental results is very good. Note here that the presence of the Bloch waves is crucial in this kind of systems: if only plane waves had been accounted for in the system, the model would not have reproduced the whole wave process because the evanescent coupling would have been neglected (see Ref. [17] and its supplementary material for more details). When the Bloch waves are considered, a perfect absorption peak appears at $f_{PA} = 800$ Hz as analytically, numerically and experimentally observed. Figure 4(b) shows the acoustic field of the full problem at the perfect absorption peak. It is worth noting here that perfect absorption is very sensible to the geometry of the resonators, and this would explain the slight discrepancies between the analytical or numerical predictions and the experimental results. The symmetric slit exhibits the symmetric Fabry-Perot mode while the antisymmetric slit exhibits the antisymmetric Fabry-Perot mode. Both modes are excited at the same frequency, i.e., the structure presents a degenerate resonance.

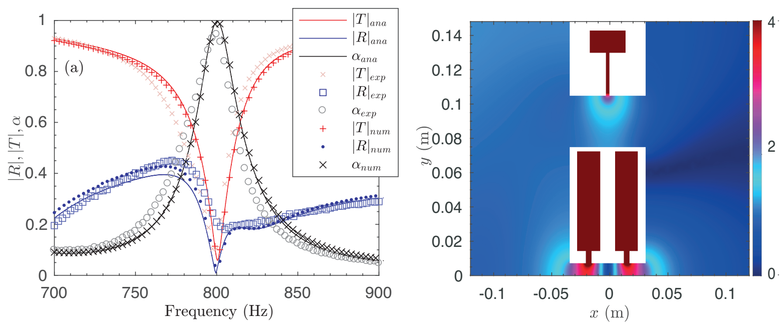

Figure 4: (a) Analytical, numerical and experimental scattering coefficients of the full problem. (b) Represents the absolute value distribution of the acoustic field at the perfect absorption of the full scattering problem. Figure adapted with permission from Ref. [17].

5 Conclusions

The conditions to obtain perfect absorption in ventilated problems with both mirror and non-mirror symmetric systems are discussed in this talk. We have shown that with non-mirror symmetric systems unidirectional perfect absorption can be obtained. For the case of mirror-symmetric system perfect absorption can be obtained by means of degenerate resonators, i.e., resonators presenting symmetric and antisymmetric resonances impedance matched at the same frequencies. Two examples of acoustic metamaterials made of Helmholtz resonators are described, showing the possibilities of both non-mirror and mirror symmetric systems. These materials are based on the concept of slow waves allowing to shift the resonances to the deep sub-wavelength regimes. The results shown in this work show the advances in the field of deep sub-wavelength absorption in the ventilated problems for airborne acoustics. They could motivate new developments to design broadband and omnidirectional deep sub-wavelength acoustic absorbers that will could transform the traditional means of both absorbing and controlling sound.

Acknowledgements

We gratefully acknowledge the Agence Nationale de la Recherche (ANR)–Research Grants Council (RGC) METARoom project (Grant No. ANR-18-CE08-0021) and the HYPERMETA project, funded under the program Étoiles Montantes of the Région Pays de la Loire. This paper is based upon work from European Cooperation in Science and Technology (COST) Action DENORMS (Designs for Noise Reducing Materials and Structures) Grant No. CA15125, supported by COST. N.J. acknowledges financial support from the Spanish Ministry of Science, Innovation, and Universities (MICINN) through the grant "Juan de la Cierva-Incorporación" (Grant No. IJC2018-037897-I).

References

[1] V. Romero-García, G. Theocharis, O. Richoux, A. Merkel, V. Tournat, and V. Pagneux. Perfect and broadband acoustic absorption by critically coupled sub-wavelength resonators. *Sci. Rep.*, 6:19519 EP –, 01 2016.

[2] N. Jiménez, W. Huang, V. Romero-García, V. Pagneux, and J.-P. Groby. Ultra-thin metamaterial for perfect and quasi-omnidirectional sound absorption. *Appl. Phys. Lett.*, 109(12):121902, 2016.

[3] V. Romero-García, G. Theocharis, O. Richoux, and V. Pagneux. Use of complex frequency plane to design broadband and sub-wavelength absorbers. *J. Acoust. Soc. Am.*, 139(6):3395–3403, 2016.

[4] A. Merkel, G. Theocharis, O. Richoux, V. Romero-García, and V. Pagneux. Control of acoustic absorption in one-dimensional scattering by resonant scatterers. *Appl. Phys. Lett.*, 107(24):244102, 2015.

[5] Noé Jiménez, Vicent Romero-García, Vincent Pagneux, and Jean-Philippe Groby. Quasiperfect absorption by subwavelength acoustic panels in transmission using accumulation of resonances due to slow sound. *Phys. Rev. B*, 95:014205, Jan 2017.

[6] Noé Jiménez, Vicent Romero-García, Vincent Pagneux, and Jean-Philippe Groby. Rainbow-trapping absorbers: Broadband, perfect and asymmetric sound absorption by subwavelength panels for transmission problems. *Sci. Rep.*, 7(1):13595, 2017.

[7] N. Jiménez, V. Romero-García, and J.-P. Groby. Perfect absorption of sound by rigidly-backed high-porous materials. *Acta Acustica united with Acustica*, 104(3):396–409, 2018.

[8] J.-P. Groby, W. Huang, A. Lardeau, and Y. Aurégan. The use of slow waves to design simple sound absorbing materials. *J. Appl. Phys.*, 117(12):124903, 2015.

[9] J.-P. Groby, R. Pommier, and Y. Aurégan. Use of slow sound to design perfect and broadband passive sound absorbing materials. *J. Acoust. Soc. Am.*, 139(4):1660–1671, 2016.

[10] V. Achilleos, O. Richoux, and G. Theocharis. Coherent perfect absorption induced by the nonlinearity of a helmholtz resonator. *J. Acoust. Soc. Am.*, 140(1):EL94–EL100, 2016.

[11] Matt Law, Lori E Greene, Justin C Johnson, Richard Saykally, and Peidong Yang. Nanowire dye-sensitized solar cells. *Nat. Mater.*, 4(6):455–459, 2005.

[12] Arnaud Derode, Philippe Roux, and Mathias Fink. Robust acoustic time reversal with high-order multiple scattering. *Phys. Rev. Lett.*, 75(23):4206, 1995.

[13] YD Chong, Li Ge, Hui Cao, and A Douglas Stone. Coherent perfect absorbers: time-reversed lasers. *Phys. Rev. Lett.*, 105(5):053901, 2010.

[14] Konstantin Y. Bliokh, Yury P. Bliokh, Valentin Freilikher, Sergey Savel'ev, and Franco Nori. Colloquium: Unusual resonators: Plasmonics, metamaterials, and random media. *Rev. Mod. Phys.*, 80(4):1201, 2008.

[15] Y.D. Chong, Li Ge, Hui Cao, and A.D. Stone. Coherent perfect absorbers: Time-reversed lasers. *Phys. Rev. Lett.*, 105:053901, 2010.

[16] J. R. Piper, Victor Liu, and Shanhui Fan. Total absorption by degenrate critical coupling. *Appl. Phys. Lett.*, 104:251110, 2014.

[17] V. Romero-García, N. Jiménez, J.-P. Groby, A. Merkel, V. Tournat, G. Theocharis, O. Richoux, and V. Pagneux. Perfect absorption in mirror-symmetric acoustic metascreens. *Phys. Rev. Applied*, 14(054055), 2020.